Pergamon

Tetrahedron 56 (2000) 1701–1706

TETRAHEDRON

Diels–Alder Reactions of a Thiazole *o*-Quinodimethane with 2- and 3-Bromo-5-hydroxynaphthoquinones. A Theoretical Study

Fernando Zuloaga,[a] Monique Domard,[b] Félix Pautet,[c] Houda Fillion[c,*] and Ricardo Tapia[d,*]

[a]*Departamento de Fisico Quimica, Facultad de Quimica, Pontificia Universidad Catolica de Chile, Casilla 306, Santiago, Chile*
[b]*Groupe de Synthèse de Molécules Bioactives, Laboratoire de Chimie Physique, Faculté de Pharmacie, Université Claude Bernard, 8, Avenue Rockefeller, F-69373 Lyon Cedex 08, France*
[c]*Groupe de Synthèse de Molécules Bioactives, Laboratoire de Chimie Organique, Faculté de Pharmacie, Université Claude Bernard, 8, Avenue Rockefeller, F-69373 Lyon Cedex 08, France*
[d]*Departamento de Quimica, Facultad de Quimica, Pontificia Universidad Catolica de Chile, Casilla 306, Santiago, Chile*

Received 20 September 1999; accepted 24 January 2000

Abstract—PM3, molecular hardness and ab initio (3-21G*) calculations were performed in order to explain the high regioselectivities observed in the Diels–Alder reactions of *o*-QDM **2** and 2- or 3-bromo-5-hydroxynaphthoquinones **3a** and **4a**. The theoretical findings of this study agree with the experimental results and support the statement that hydrogen bonding plays a crucial role on the regiocontrol of the cycloadditions.

The Diels–Alder reaction of *o*-quinodimethane (*o*-QDM) with dienophiles has proven to be an efficient and powerful method to build polycyclic aromatic compounds.[1] The heterocyclic analogues of *o*-QDM have received considerable attention because of the development of very mild methods to generate these highly reactive dienes.[2] Recently, we described the generation and Diels–Alder trapping of 4-methylene-5-(bromomethylene)-4,5-dihydrothiazole **2** with 2- and 3-bromonaphthoquinones **3** and **4**.[3] The experimental results for these Diels–Alder reactions show that **5a** or **5b** are the major final products resulting from 2-bromonaphthoquinones **3a** or **3b** used respectively as the starting materials. On the other hand, it turns out experimentally that **6a** or **6b** are the major products when 3-bromonaphthoquinones **4a** or **4b** were used as dienophiles (Scheme 1 and Table 1).

Frontier molecular orbital (FMO) method at the semiempirical PM3 level theory has been used to analyse the behavior of (*Z*) *o*-QDM **2** in these cycloaddition reactions. The results indicated that the larger coefficient for the HOMO orbital was found at the carbon atom bearing a bromine atom (Scheme 2). In the case of the bromonaphthoquinones **3a** (*syn*) and **4a** (*syn*) in which a hydrogen bond may exist between the *peri*-OH group and the carbonyl at C-4, as it is known for juglone **7** (*syn*), the calculations indicated that the larger LUMO coefficients were always located at C-2. However, the regiochemistries of the cycloadditions between *o*-QDM **2** and **3a**, on one hand, or **4a**, on the other hand, were opposite. In the case of **2** and **3a** (*syn*), the FMO theory agreed with the formation of **5a** as major product but, with **4a** (*syn*), the experimental result disagreed with the calculations since **6a** was the major adduct. The hypothesis that formation of **6a** could result from the cycloaddition of **2** and the *anti* isomer of **4a** seemed very attractive to us. We therefore undertook a theoretical study of these Diels–Alder reactions.

Theory and Methods

The PM3 method[4] was used extensively in this study because it has been proved to be accurate in predicting the reactivity and regioselectivity of Diels–Alder reactions.[5] The coefficients of the frontier molecular orbitals were calculated using MOPAC of the SYBYL program. Optimized geometries for products, intermediates and transition state structures considered here were calculated at the PM3 level, but ab initio calculations (3-21G*) were performed in some cases to improve activation energies, since it is well known that semiempirical energy differences of 1–2 kcal are not reliable.[6] These calculations were performed using Spartan.[7] Vibrational analysis was also done for each transition structure thus obtaining only one imaginary vibrational frequency corresponding to the formation of new bonds. The activation energies were obtained from ab initio methods (at the 3-21G* level) on the PM3 optimized geometries.

Keywords: Diels–Alder; thiazole *o*-quinodimethane; bromojuglone; hardness calculation; transition state.

* Corresponding authors. Tel.: +33-4-78-77-71-38; fax: +33-4-78-77-71-58; e-mail: fillion@cismsun.univ-lyon1.fr; Tel.: +56-2-686-4429; fax: +56-2-686-4744; e-mail: rtapia@puc.cl

0040–4020/00/$ - see front matter
PII: S0040-4020(00)00066-1

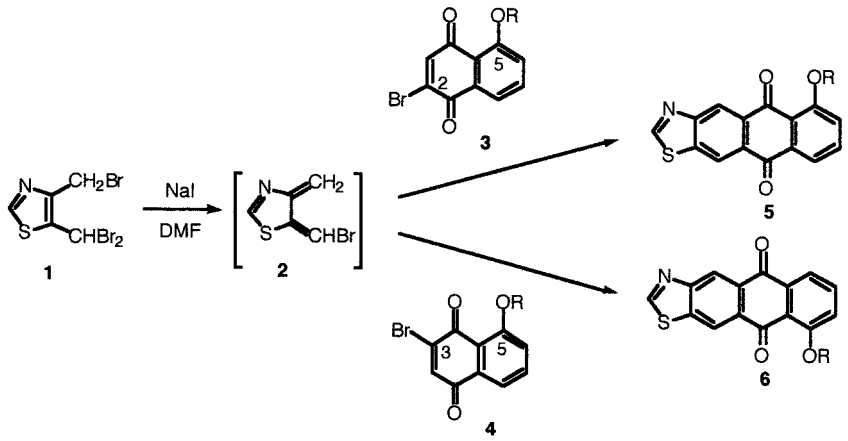

Scheme 1. **3a**, **4a**, **5a**, **6a**: R=H; **3b**, **4b**, **5b**, **6b**: R=$COCH_3$

Table 1. Regiochemistry of the cycloadditions of **2** with quinones **7**, **3** and **4**

Quinone	Products	Ratio 5/6
7	**5a**+**6a**	70/30
3a	**5a**+**6a**	92/08
4a	**5a**+**6a**	08/92
3b	**5b**+**6b**	95/05
4b	**5b**+**6b**	05/95

The Hard and Soft Acids and Bases Principle (HSAB) has also been invoked in a local sense to account, in terms of the density functional theory (DFT), for the response of the chemical system to different kinds of reagents. The local use of the general behavior 'soft likes soft' and 'hard likes hard', together with the idea that the larger the value of the local site Fukui function, the greater its reactivity, seems to be a very good approach to explain the chemical reactivity of a wide variety of systems.[8] However, we plan here to make use of the molecular hardness change in order to study the potential chemical attack at different sites of one molecule to another one.[9] Obviously, one of them will be the acid (the electron-acceptor) and the other must play the role of the base (the electron-donor). We can see that this strategy is very useful when the various electronic and steric effects of substituents and heteroatoms might make predictions of reaction sites difficult.

For a molecular system made of electrons and nuclei reaching an equilibrium state, the electronegativity χ and the absolute hardness η are written as derivatives of the electronic energy with respect to the number of electrons

$$\chi = -\left(\frac{\partial E}{\partial N}\right)_{\mathrm{v}} = \frac{I+A}{2},\ \eta = \frac{1}{2}\left.\frac{\partial \chi}{\partial N}\right|_{\mathrm{v}} \tag{1}$$

In DFT Koopmans' theorem is obeyed for the highest occupied level so that I and A are replaced by the HOMO and LUMO energies. The isosurface for the electrostatic potential and the electronegativity surface map for the molecule were drawn following a similar principle already stated elsewhere.[8] Briefly, the electrostatic potential $\phi(\mathbf{r})$ that the electrons and nuclei of a molecule create at each point $\mathbf{r}$ in the surrounding space is given rigorously by Eq. 2

$$\phi(\mathbf{r}) = \sum_{\mathrm{A}} \frac{Z_{\mathrm{A}}}{|\mathbf{R}_{\mathrm{A}} - \mathbf{r}|} - \int \frac{\rho(\mathbf{r}')\,\mathrm{d}\mathbf{r}'}{|\mathbf{r}' - \mathbf{r}|} \tag{2}$$

where Z_{A} is the charge on nucleus A located at $\mathbf{R}_{\mathrm{A}}$, and $\rho(\mathbf{r})$ is the electronic density function of the molecule,

$$\rho(\mathbf{r}) = \sum_{i=1}^{\mathrm{occ}} n_i |\psi_i(\mathbf{r})|^2$$

for each occupied molecular orbital $\psi_i(\mathbf{r})$. Interestingly, $\phi(\mathbf{r})$ is a real physical property derived from diffraction

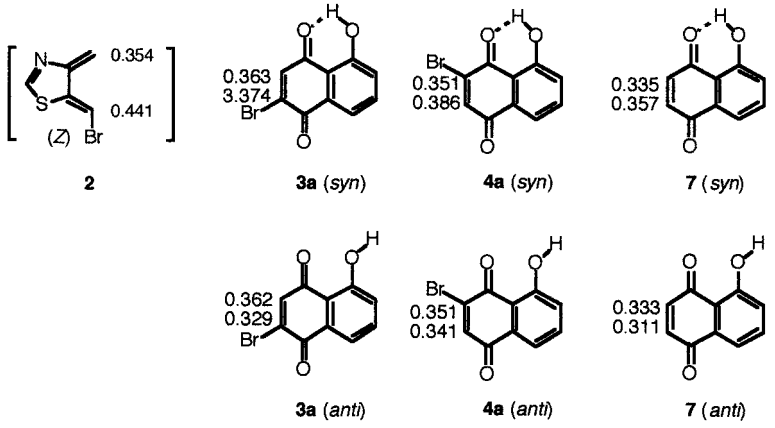

Scheme 2.

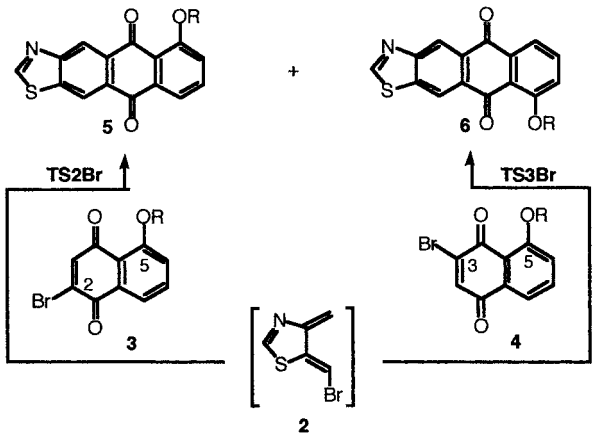

Scheme 3.

experiments and any molecular reactivity index derived from it will correspond also to useful experimental parameters. In DFT the molecular electrostatic potential $\phi(\mathbf{r})$ is directly related[10] to the molecular electronegativity and since the latter is constant within the molecular space, there exists a set of $\mathbf{r}_\chi$ position values at which the equality

$$\chi = \sum_{\mathrm{A}} \frac{Z_{\mathrm{A}}}{|\mathbf{R}_{\mathrm{A}} - \mathbf{r}|} - \int \frac{\rho(\mathbf{r}')\,\mathrm{d}\mathbf{r}'}{|\mathbf{r}' - \mathbf{r}|}; \qquad \mathbf{r} = \text{set}\,\{\mathbf{r}_\chi\} \tag{3}$$

is obeyed. This defines the electronegativity surface map for the molecule. In addition, its derivative against the number of electrons N at $\{\mathbf{r}_\chi\}$ yields the molecular hardness as a surface map for each value of χ at the set $\{\mathbf{r}_\chi\}$

$$\left.\frac{\partial \chi}{\partial N}\right|_v = \int \frac{\rho_{\text{frontier}}(r')\,\mathrm{d}r'}{|r' - r_\chi|} = 2\eta_{\text{frontier}}(\mathbf{r}_\chi) \tag{4}$$

Two possible phenomena were analyzed: (a) an electrophilic attack over the molecule (thereby HOMO is involved for the δN electron transfer process) yielding $2\eta_-(\mathbf{r}_\chi)$ and (b) a nucleophilic attack (LUMO involved) yielding $2\eta_+(\mathbf{r}_\chi)$. Equation (4) establishes that the frontier orbital electrostatic potential at different values of $\mathbf{r}_\chi$ is a measure of the hardness achieved by the molecule in response to a perturbation represented by the chemical attack of an electrophile or nucleophile, respectively. By this procedure a contour surface for η encoded to χ around the molecule was built to learn about which site yields the hardest molecular value for a given chemical attack. These statements conform with the maximum hardness principle[9–13] already stated that has been invoked to deduce regiospecificity in Diels–Alder reactions.

Results and Discussion

We plan to use these concepts to predict the regiochemistry of the Diels–Alder reaction of 2-bromonaphthoquinone and 3-bromonaphthoquinone derivatives **3** and **4** with 4-methylene-5-(bromomethylene)-4,5-dihydrothiazole **2** shown in Scheme 1. The rate-determining step for the reaction is the formation of a space charge separation in which the Transition State (TS) strongly resembles the intermediate. Initially, these steps are (with few exceptions) rapid and reversible so that the formation of various isomers is dependent on the activation energy necessary to form the appropriate intermediate complex (Scheme 3).

It is important to realize at this point that the molecular electronegativity χ, by its definition, is a unique property at any given region of the molecule. A plot of the molecular hardness expressed as the frontier orbital electrostatic potential of Eq. 4 coded at the 115.46 kcal/mol isosurface electronegativity value for *o*-QDM **2** is given in Fig. 1. The values shown are the hardness achieved by the molecule when an electrophile performs a chemical attack at the 5-bromomethylene or at the 4-methylene site. The results indicate that a higher value for hardness is obtained when the electrophile approaches the bromo-derivatized carbon near to the S-atom heterocycle. All these calculations, performed at the PM3 level theory, show that **2** provides two rather well differentiated sites for Diels–Alder reactions.

Fig. 2 shows similar results for the acceptor molecules **3a** (*syn*) and **4a** (*syn*) and though there is not a large difference between the two sites for 2-bromonaphthoquinone **3a** (*syn*), one finds that the C-2 site is slightly harder against a nucleophile so that the product **5a** is the main regioisomer of the reaction. In contrast, for the **3a** (*anti*) (Fig. 3), the influence of lack of hydrogen bonding is negligible to differentiate conclusively among C-2 and C-3 (168.8 and 169.9 kcal hardness values, respectively)

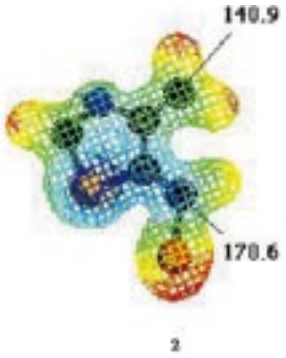

Figure 1. Hardness map for bromomethylene dihydrothiazole donor molecule **2** encoded at the isosurface value of 115.46 kcal/mol for the molecular electronegativity.

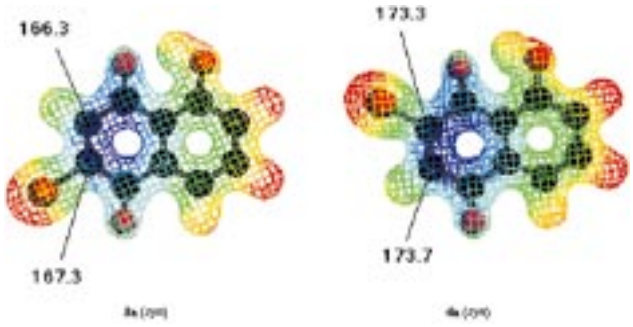

Figure 2. Hardness maps for 2-bromonaphthoquinone **3a** (*syn*) and 3-bromonaphthoquinone **4a** (*syn*), each encoded one at the isosurface value of 133.4 kcal/mol for the molecular electronegativity.

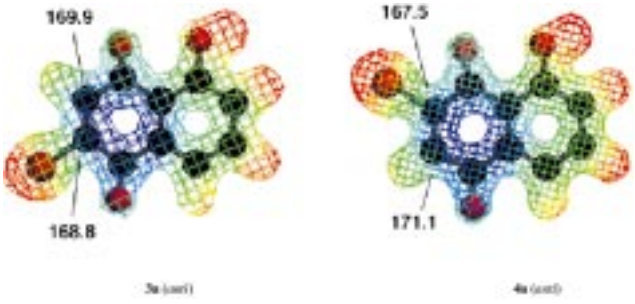

Figure 3. Hardness maps for 2-bromonaphthoquinone **3a** (*anti*) and 3-bromonaphthoquinone **4a** (*anti*), each encoded at the isosurface value of 130.3 kcal/mol for the molecular electronegativity.

sites thereby preferential regioselectivity against **2** is not clear, unless one invokes that for **3a** (*syn*) its total energy is 15.8 kcal/mol more stable than **3a** (*anti*) in the ground state meaning that hydrogen bonding is present during the cycloaddition reaction.

On the other hand, hardness difference is smaller when analyzing the results for 3-bromonaphthoquinone **4a** (*syn*). Again, C-2 is 0.4 kcal/mol harder than C-3 against a nucleophile. However, in the case of **4a** (*anti*) (Fig. 3) the hydrogen arrangement induces large changes in geometry yielding C-2 definitely harder than C-3 (171.1 and 167.5 hardness values, respectively). Considering the reaction of **2** with **4a** (*anti*), the predicted regioisomer **5a** is in disagreement with experiments. In fact, hydrogen bonding effects, shown in Fig. 2 for **3a** (*syn*) and **4a** (*syn*), force both molecules to be planar so there are no differences among them for the adduct formation from either backside or frontside attack by the donor molecule. The absence of hydrogen bonding drastically changes the molecular geometry thus allowing both alternatives for adduct formation.

So, we have calculated hardness for the acetyl derivatives **3b** and **4b** (Fig. 4). Before discussing the reactivity indexes results, it is important to describe the kind of distortion that **3b** and **4b** have acquired. Both carbonyl groups of the quinone system have moved outward, the aromatic rings are bent among them and the bromine atom has also moved outward. These findings yield different hardness values depending upon whether one measures them from above or below the molecular plane. The values shown in Fig. 4 have been obtained from above the twisted molecular planes

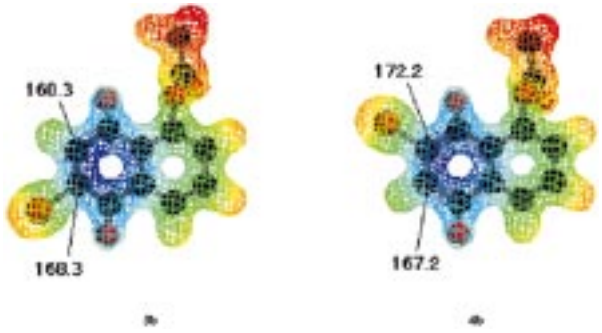

Figure 4. Hardness maps for 2-bromo-5-acetoxynaphthoquinone **3b** and 3-bromo-5-acetoxynaphthoquinone **4b** encoded at the isosurface value of 136.7 and 137.1 kcal/mol, respectively, for the molecular electronegativity.

since they are higher than the values measured from below the plane. It is seen that for **3b**, hardness has changed drastically to render C-2 the hardest site for a nucleophilic attack while C-3 is the hardest one for **4b**. Since hydrogen bonding effects are missing for the acetylated derivatives, hardness values in Fig. 4 are drastically different from those shown in Fig. 2. It turns out that the principle of maximum hardness results in the Diels–Alder reaction of **2** with 2-bromo-5-acetoxynaphthoquinone **3b** yielding the acetylated cycloadduct **5b** as the main product whereas its reaction with 3-bromo-5-acetoxynaphthoquinone **4b** affords **6b**, in agreement with experimental results. The position of the bromine substituent at C-2 or C-3 in naphthoquinones **3b** and **4b** is playing an important role here in the regiocontrol of the Diels–Alder reactions.

Let us now focus our attention on the transition states of intermediates of Scheme 1 that play a role in the reaction mechanism involved to corroborate our findings. Fig. 5 and 6 show the main features for the transition state (TS) structures found in this study. Each TS adduct was generated by assuming that a concerted reaction mechanism is

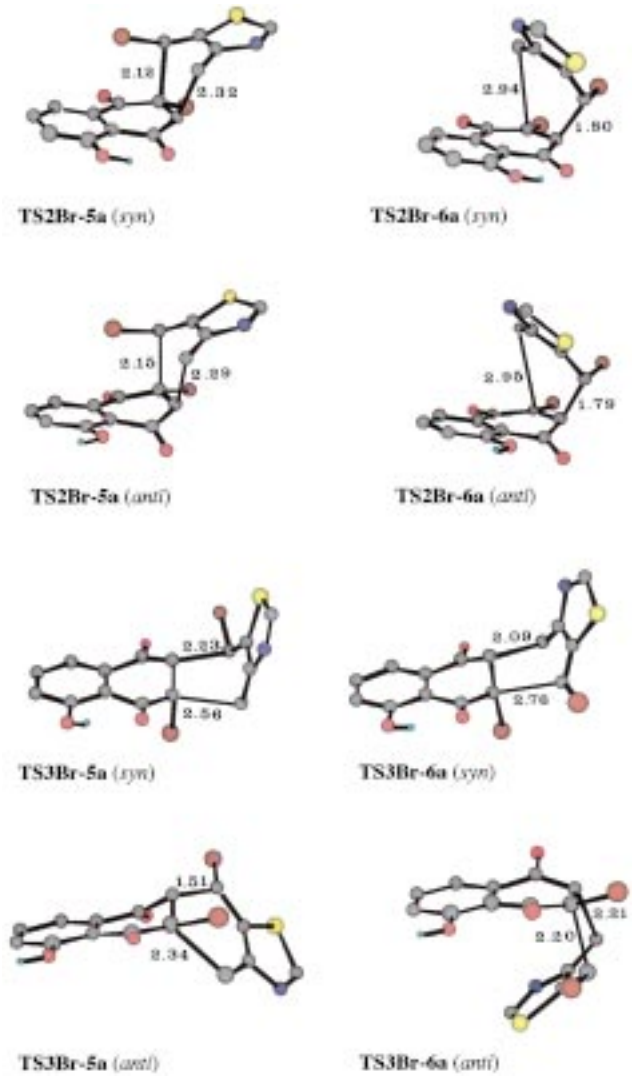

Figure 5. Transition states of the cycloadditions between *o*-QDM **2** and 2- or 3-bromo-5-hydroxynaphthoquinones **3a** or **4a**, respectively.

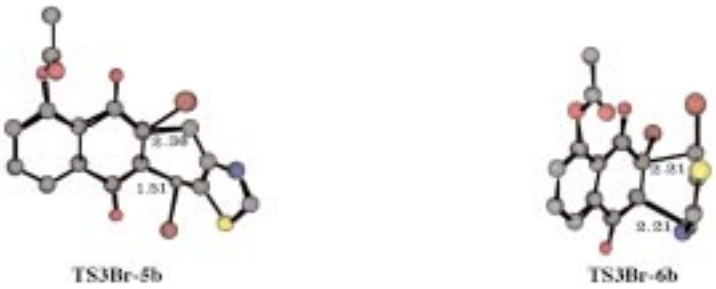

Figure 6. Transition states of the cycloadditions between *o*-QDM **2** and 2- or 3-bromo-5-acetoxynaphthoquinones **3b** or **4b**, respectively.

obeyed, as studied elswhere for the Diels–Alder reaction of disubstituted cyclohexadienones.[14] Furthermore, transition structure geometry for each of them was optimized by using PM3 methods[4] as described before and making a vibrational analysis to verify that only one imaginary vibrational mode was present and assigned to the new C–C bonds formation for the intermediate TS structure. Bond distances achieved are given explicitly in Figs. 5 and 6 so that one can easily recognize that the reaction mechanisms are concerted but asynchronous. In fact, the transition structure made up by 3-bromo-5-hydroxynaphthoquinone **4a** and 3-bromo-5-acetoxynaphthoquinone **4b** and *o*-QDM **2** [**TS3Br-6a** (*anti*) and **TS3Br-6b**] are the only ones that appear to be concerted Diels–Alder cycloadditions of synchronous type. Moreover, Fig. 5 shows that for 2-bromonaphthoquinone **3a** (*syn*) there is indeed hydrogen bond formation between the *peri*-OH group and the oxygen atom of carbonyl at C-4, where the H···O (quinonic) bond distance is 1.83 Å for any of the **TS2Br-5a** (*syn*) and **TS2Br-6a** (*syn*) achieved. A similar situation was observed for **TS3Br-5a** (*syn*) and **TS3Br-6a** (*syn*).

Let us now discuss the geometry achieved by TS molecules. It is important to notice that PM3 activation energies (Table 2) are not reliable when comparing some of the different molecular geometries, due to the fact that some energy differences are not large enough. However, for those cases where activation energy differences are significant, PM3 values follow the same trend than ab initio results. To begin with, 2-bromonaphthoquinones transition state adducts with **2** are rather twisted and folded among the rings whereas this is not the case for 3-bromonaphthoquinones. These geometrical features are important when analyzing the regioselectivity of the reaction products. Probably, the energy barrier values for the transition states shown in Table 2 have taken these facts into account. The transition state structure **TS2Br-5a** for 2-bromonaphthoquinone **3a** (*syn*) (entry 1) has a lower energy barrier [ab-initio 3-21G* level] than **TS2Br-6a** (entry 2) thus yielding **5a** as the major product of the reaction. These results are more definite than the previously discussed hardness analysis. Moreover, the *anti*-OH bonding conformation does not have any appreciable effect on the energy barrier (entries 3 and 4).

For the 3-bromonaphthoquinone **4a** case, things are completely different. Hardness difference among C-2 and C-3 sites that was found to be non-significant for the *syn* conformation does not show appreciable difference in activation energies for the **TS3Br** transition structure leading to **5a** or **6a** (entries 5 and 6). In contrast, the TS through **TS3Br** path activation energies for **4a** (*anti*) does provide enough evidence to assess the formation of **6a** as the major product in agreement with experimental results (entry 8).

On the other hand, 3-bromonaphthoquinone **4b** represents the case in which H-bonding effects are not present. The hardness map of Fig. 4 shows that C-3 has become the hardest site yielding **6b** as the major product of the reaction. These findings agree with [3-21G*] activation barrier values given in Table 2 (entry 10).

Finally, the above theoretical results agree completely with those experimentally observed and support the above mentioned statement that hydrogen bonding effects play a crucial role on the regiochemistry of the Diels–Alder reactions discussed here.

Table 2. Predicted activation energies (kcal/mol) and regioselective preferences

Entry	Quinone	Transition state	Activation energy		Major product
			PM3	3-21G*[a]	
1	**3a** (*syn*)	**TS2Br-5a** (*syn*)	27.8	47.3	**5a**
2		**TS2Br-6a** (*syn*)	27.7	72.0	
3	**3a** (*anti*)	**TS2Br-5a** (*anti*)	33.4	48.1	**5a**
4		**TS2Br-6a** (*anti*)	33.7	63.4	
5	**4a** (*syn*)	**TS3Br-5a** (*syn*)	66.2	81.5	
6		**TS3Br-6a** (*syn*)	65.1	84.8	**6a**
7	**4a** (*anti*)	**TS3Br-5a** (*anti*)	48.6	82.9	
8		**TS3Br-6a** (*anti*)	32.0	34.4	**6a**
9	**4b**	**TS3Br-5b**	47.5	79.7	
10		**TS3Br-6b**	32.8	35.9	**6b**

[a] Ab initio 3-21G* results at the PM3 optimized TS geometry.

References

1. For a review, see: Segura, J. L.; Martin, N. *Chem. Rev.* **1999**, *99*, 3199–3246.
2. For reviews, see: (a) Chou, T.-S. *Rev. Heteroat. Chem.* **1993**, *8*, 65–104. (b) Collier, S. J.; Storr, R. C. In *Progress in Heterocyclic Chemistry*; G. W. Gribble, T. L. Gilchrist Eds.; Pergamon: The Netherlands, 1998; Vol. 10, pp 25–48.
3. Al Hariri, M.; Jouve, K.; Pautet, F.; Domard, M.; Fenet, B.; Fillion, H. *J. Org. Chem.* **1997**, *62*, 405–410.
4. Stewart, J. *J. Comp. Chem.* **1989**, *10*, 209–221.
5. Jursic, B. S.; Zadrowsky, Z. *Tetrahedron* **1994**, *50*, 10379–10390; Jursic, B. S.; Zadrowsky, Z. *J. Hetrocyclic Chem.* **1994**, *31*, 1429–1432.
6. Trong Anh, N.; Frison, G.; Solladié-Cavallo, A.; Metzner, P. *Tetrahedron* **1998**, *54*, 12841–12852.
7. Spartan version 5.0.3; Wavefunction Inc., 1998.
8. Gazquez, J. L.; Mendez, F. *J. Phys. Chem.* **1994**, *98*, 4591–4593.
9. Zuloaga, F.; Tapia, R.; Quintanar, C. *J. Chem. Soc., Perkin Trans. 2* **1995**, 939–943.
10. Lopez, R.; Boys, D.; Loeb, B.; Zuloaga, F. *J. Chem. Soc., Perkin Trans. 2* **1998**, 877–883.
11. Damoun, S.; Van de Woude, G.; Mendez, F.; Geerlings, P. *J. Phys. Chem. A* **1997**, *101*, 886–893.
12. Pearson, R. G. *Proc. Nat. Acad. Sci.* **1986**, *83*, 8440–8441; Pearson, R. G. *Acc. Chem. Res.* **1993**, *26*, 250–255.
13. Parr, R. G.; Chattaraj, P. K. *J. Am. Chem. Soc.* **1991**, *131*, 1854–1855.
14. Silvero, G.; Lucero, M. J.; Winterfeldt, E.; Houk, K. N. *Tetrahedron* **1998**, *54*, 7293–7300.